

Observation of the $\Lambda_b^0 \rightarrow \chi_{c1}(3872)pK^-$ decay



The LHCb collaboration

E-mail: Ivan.Belyaev@itep.ru

ABSTRACT: Using proton-proton collision data, collected with the LHCb detector and corresponding to 1.0, 2.0 and 1.9 fb⁻¹ of integrated luminosity at the centre-of-mass energies of 7, 8, and 13 TeV, respectively, the decay $\Lambda_b^0 \rightarrow \chi_{c1}(3872)pK^-$ with $\chi_{c1}(3872) \rightarrow J/\psi \pi^+\pi^-$ is observed for the first time. The significance of the observed signal is in excess of seven standard deviations. It is found that (58 ± 15)% of the decays proceed via the two-body intermediate state $\chi_{c1}(3872)\Lambda(1520)$. The branching fraction with respect to that of the $\Lambda_b^0 \rightarrow \psi(2S)pK^-$ decay mode, where the $\psi(2S)$ meson is reconstructed in the $J/\psi \pi^+\pi^-$ final state, is measured to be:

$$\frac{\mathcal{B}(\Lambda_b^0 \rightarrow \chi_{c1}(3872)pK^-)}{\mathcal{B}(\Lambda_b^0 \rightarrow \psi(2S)pK^-)} \times \frac{\mathcal{B}(\chi_{c1}(3872) \rightarrow J/\psi \pi^+\pi^-)}{\mathcal{B}(\psi(2S) \rightarrow J/\psi \pi^+\pi^-)} = (5.4 \pm 1.1 \pm 0.2) \times 10^{-2},$$

where the first uncertainty is statistical and the second is systematic.

KEYWORDS: B physics, Branching fraction, Exotics, Hadron-Hadron scattering (experiments)

ARXIV EPRINT: [1907.00954](https://arxiv.org/abs/1907.00954)

Contents

1	Introduction	1
2	Detector and simulation	2
3	Event selection	3
4	Signal yields and efficiencies	4
5	Systematic uncertainties	6
6	Results and summary	8
	The LHCb collaboration	14

1 Introduction

The $\chi_{c1}(3872)$ state, also known as $X(3872)$, was observed in 2003 by the Belle collaboration [1] and subsequently confirmed by several other experiments [2–7]. This discovery has attracted much interest in exotic charmonium spectroscopy since it was the first observation of an unexpected charmonium candidate. The mass of the $\chi_{c1}(3872)$ state has been precisely measured [5, 8] and the dipion mass spectrum in the decay $\chi_{c1}(3872) \rightarrow J/\psi \pi^+ \pi^-$ was also studied [1, 6, 9]. The quantum numbers of the state were determined to be $J^{PC} = 1^{++}$ from measurements performed by the LHCb collaboration [10].

Despite a large amount of experimental information, the nature of the $\chi_{c1}(3872)$ particle is still unclear [11, 12]. It has been interpreted as a $\chi_{c1}(2P)$ charmonium state [13, 14], molecular state [15–17], tetraquark [18, 19], $c\bar{c}g$ hybrid meson [20], vector glueball [21] or mixed state [22, 23]. Studies of radiative $\chi_{c1}(3872)$ decays [24–26] have reduced the number of possible interpretations of this state [27–29]. Thus far, the $\chi_{c1}(3872)$ particle has been widely studied in prompt hadroproduction [2, 5–7] and in the weak decays of beauty mesons. Several decays of the Λ_b^0 baryon to charmonium have been observed [30–37]. Observing Λ_b^0 decays involving the $\chi_{c1}(3872)$ state will allow comparison of their decay rates to the rates for conventional charmonium states, where, for instance, factorisation and spectator quarks assumptions may lead to different results depending on the nature of the $\chi_{c1}(3872)$ state.

In this paper the first observation of the $\chi_{c1}(3872)$ state in the beauty-baryon decay $\Lambda_b^0 \rightarrow \chi_{c1}(3872) p K^-$ is reported. This study is based on data collected with the LHCb detector in proton-proton (pp) collisions corresponding to 1.0, 2.0 and 1.9 fb^{-1} of integrated

luminosity at centre-of-mass energies of 7, 8 and 13 TeV, respectively. A measurement of the $\Lambda_b^0 \rightarrow \chi_{c1}(3872)pK^-$ branching fraction relative to that of the $\Lambda_b^0 \rightarrow \psi(2S)pK^-$ decay,

$$R = \frac{\mathcal{B}(\Lambda_b^0 \rightarrow \chi_{c1}(3872)pK^-)}{\mathcal{B}(\Lambda_b^0 \rightarrow \psi(2S)pK^-)} \times \frac{\mathcal{B}(\chi_{c1}(3872) \rightarrow J/\psi \pi^+ \pi^-)}{\mathcal{B}(\psi(2S) \rightarrow J/\psi \pi^+ \pi^-)}, \quad (1.1)$$

is performed, where the $\chi_{c1}(3872)$ and $\psi(2S)$ mesons are reconstructed in the $J/\psi \pi^+ \pi^-$ final state. Throughout this paper the inclusion of charge-conjugated processes is implied.

2 Detector and simulation

The LHCb detector [38, 39] is a single-arm forward spectrometer covering the pseudorapidity range $2 < \eta < 5$, designed for the study of particles containing b or c quarks. The detector includes a high-precision tracking system consisting of a silicon-strip vertex detector surrounding the pp interaction region [40], a large-area silicon-strip detector located upstream of a dipole magnet with a bending power of about 4 Tm, and three stations of silicon-strip detectors and straw drift tubes [41, 42] placed downstream of the magnet. The tracking system provides a measurement of the momentum of charged particles with a relative uncertainty that varies from 0.5% at low momentum to 1.0% at 200 GeV/c. The minimum distance of a track to a primary vertex (PV), the impact parameter (IP), is measured with a resolution of $(15 + 29/p_T) \mu\text{m}$, where p_T is the component of the momentum transverse to the beam, in GeV/c. Different types of charged hadrons are distinguished using information from two ring-imaging Cherenkov detectors (RICH) [43]. Photons, electrons and hadrons are identified by a calorimeter system consisting of scintillating-pad and preshower detectors, an electromagnetic and a hadronic calorimeter. Muons are identified by a system composed of alternating layers of iron and multiwire proportional chambers [44].

The online event selection is performed by a trigger [45], which consists of a hardware stage, based on information from the calorimeter and muon systems, followed by a software stage, which applies a full event reconstruction. At the hardware trigger stage, events are required to have a muon with high p_T or a pair of opposite-sign muons with a requirement on the product of muon transverse momenta, or a hadron, photon or electron with high transverse energy in the calorimeters. The software trigger requires two muons of opposite charge forming a good-quality secondary vertex with a mass in excess of $2.7 \text{ GeV}/c^2$, or a two-, three- or four-track secondary vertex with at least one charged particle with a large p_T and inconsistent with originating from any PV. For both cases significant displacement of the secondary vertex from any primary pp interaction vertex is required.

Simulated events are used to describe the signal mass shapes and compute efficiencies. In the simulation, pp collisions are generated using PYTHIA [46] with a specific LHCb configuration [47]. Decays of unstable particles are described by EVTGEN package [48], in which final-state radiation is generated using PHOTOS [49]. The interaction of the generated particles with the detector, and its response, are implemented using the GEANT4 toolkit [50, 51] as described in ref. [52].

3 Event selection

The $\Lambda_b^0 \rightarrow J/\psi \pi^+ \pi^- p K^-$ candidate decays are reconstructed using $J/\psi \rightarrow \mu^+ \mu^-$ decay mode. To separate signal from background, a loose preselection is applied, as done in ref. [32], followed by a multivariate classifier based on a Boosted Decision Tree with gradient boosting (BDTG) [53].

Muon, proton, pion and kaon candidates are identified using combined information from the RICH, calorimeter and muon detectors. They are required to have a transverse momentum larger than 550 MeV/c for muon and 200 MeV/c for hadron candidates. To allow for efficient particle identification, kaons and pions are required to have a momentum between 3.2 and 150 GeV/c, whilst protons must have a momentum between 10 and 150 GeV/c. To reduce the combinatorial background, only tracks that are inconsistent with originating from any PV are used.

Pairs of oppositely charged muons consistent with originating from a common vertex are combined to form $J/\psi \rightarrow \mu^+ \mu^-$ candidates. The mass of the pair is required to be between 3.0 and 3.2 GeV/c².

To form Λ_b^0 candidates, the selected J/ψ candidates are combined with a pair of oppositely charged pions, a proton and a negatively charged kaon. Each Λ_b^0 candidate is associated with the PV that yields the smallest χ_{IP}^2 , where χ_{IP}^2 is defined as the difference in the vertex-fit χ^2 of a given PV reconstructed with and without the particle under consideration. The χ_{IP}^2 value is required to be less than 9. To improve the Λ_b^0 mass resolution a kinematic fit [54] is performed. This fit constrains the mass of the $\mu^+ \mu^-$ pair to the known mass of the J/ψ meson [55]. It is also required that the Λ_b^0 momentum vector points back to the associated pp interaction vertex. In addition, the measured decay time of the Λ_b^0 candidate, calculated with respect to the associated PV, is required to be greater than 75 $\mu\text{m}/c$ to suppress poorly reconstructed candidates and background from particles originating from the PV.

To further suppress cross-feed from the $B^0 \rightarrow J/\psi \pi^+ \pi^- \pi^+ K^-$ decay with a positively charged pion misidentified as a proton, a veto is applied on the Λ_b^0 mass, recalculated with a pion mass hypothesis for the proton. A similar veto is applied to suppress $B_s^0 \rightarrow J/\psi \pi^+ \pi^- K^+ K^-$ decays. Any candidate with a recalculated mass consistent with the known B^0 or B_s^0 mass is rejected.

A BDTG is used to further suppress the combinatorial background. It is trained on a simulated sample of $\Lambda_b^0 \rightarrow \chi_{c1}(3872) p K^-$, $\chi_{c1}(3872) \rightarrow J/\psi \pi^+ \pi^-$ decays for the signal, while for background the high-mass data sideband is used, defined as $m_{J/\psi \pi^+ \pi^- p K^-} > 5640 \text{ MeV}/c^2$, where the regions of $m_{J/\psi \pi^+ \pi^-}$ populated by $\psi(2S) \rightarrow J/\psi \pi^+ \pi^-$ and $\chi_{c1}(3872) \rightarrow J/\psi \pi^+ \pi^-$ decays are excluded. The k -fold cross-validation technique [56] is used in the BDTG training, in which the candidates are pseudo-randomly split into $k = 23$ samples. The BDTG applied to a particular sample is trained using all the data from the other 22, allowing $\sim 95\%$ of the total sample to be used for each training with no need to remove the candidates used from the final data set. The outputs of all multivariate classifiers are consistent. The BDTG is trained on variables related to reconstruction quality, kinematics, lifetime of Λ_b^0 candidates, the value of χ^2 from the kinematic fit described above, and the mass of the dipion combination.

The simulated samples are corrected to better match the kinematic distributions observed in data. The transverse momentum and rapidity distributions and the lifetime of the Λ_b^0 baryons in simulated samples are adjusted to match those observed in a high-yield low-background sample of $\Lambda_b^0 \rightarrow J/\psi pK^-$ decays. Finally, the simulated events are weighted to match the particle identification efficiencies determined from data using calibration samples of low-background decays: $D^{*+} \rightarrow D^0(\rightarrow K^-\pi^+)\pi^+$, $K_S^0 \rightarrow \pi^+\pi^-$, $D_s^+ \rightarrow \phi(\rightarrow K^+K^-)\pi^+$, for kaons and pions; and $\Lambda \rightarrow p\pi^-$ and $\Lambda_c^+ \rightarrow pK^+\pi^-$ for protons [43, 57]. The simulated decays of Λ_b^0 baryons are produced according to a phase-space decay model. The $\chi_{c1}(3872) \rightarrow J/\psi \pi^+\pi^-$ decay proceeds via the $J/\psi \rho^0$ S-wave intermediate state [10]. The simulated $\Lambda_b^0 \rightarrow \psi(2S)pK^-$ decays are corrected to reproduce the pK^- mass and $\cos\theta_{pK^-}$ distributions observed in data, where the helicity angle of the pK^- system, θ_{pK^-} , is defined as the angle between the momentum vectors of the kaon and Λ_b^0 baryon in the pK^- rest frame. To account for imperfections in the simulation of charged particle reconstruction, efficiency corrections obtained using data are also applied [58].

The requirement on the BDTG output t is chosen to maximize the Punzi figure of merit $\epsilon_t/(\alpha/2 + \sqrt{B_t})$ [59], where ϵ_t is the signal efficiency for the $\Lambda_b^0 \rightarrow \chi_{c1}(3872)pK^-$ decay obtained from the simulation, $\alpha = 5$ is the target signal significance in units of standard deviations, B_t is the expected background yield within narrow mass windows centred on the known Λ_b^0 and $\chi_{c1}(3872)$ masses [55].

4 Signal yields and efficiencies

The yields for signal and normalization channels are determined using a two-dimensional unbinned extended maximum-likelihood fit to the $J/\psi \pi^+\pi^- pK^-$ and $J/\psi \pi^+\pi^-$ masses. The probability density function used in the fit consists of four components to describe the mass spectrum:

- a signal component, describing the true $\Lambda_b^0 \rightarrow \psi_{\pi\pi} pK^-$ decays, where $\psi_{\pi\pi}$ denotes either $\psi(2S)$ or $\chi_{c1}(3872)$ final states;
- a component describing nonresonant (NR) $\Lambda_b^0 \rightarrow J/\psi \pi^+\pi^- pK^-$ decays with no intermediate $\psi_{\pi\pi}$ state;
- a component describing random combinations of $\psi_{\pi\pi}$ with pK^- pairs that are not Λ_b^0 decay products;
- and a combinatorial $J/\psi \pi^+\pi^- pK^-$ component.

The templates for the Λ_b^0 , $\chi_{c1}(3872)$ and $\psi(2S)$ signals are described by modified Gaussian functions with power-law tails on both sides [60]. The tail parameters are fixed to values obtained from simulation, while the peak positions of the Gaussian functions are free to vary in the fit. The mass resolution of the $\psi(2S)$ meson is allowed to vary in the fit, while that of the $\chi_{c1}(3872)$ signal, due to its lower yield, is fixed to the value determined from simulation and corrected by the data-simulation ratio of the mass resolutions for the $\psi(2S)$

meson. The $\Lambda_b^0 \rightarrow \psi_{\pi\pi} pK^-$ component is described by the product of the Λ_b^0 and $\psi_{\pi\pi}$ signal templates, $S_{\Lambda_b^0}(m_{J/\psi \pi^+ \pi^- pK^-}) \times S_{\psi_{\pi\pi}}(m_{J/\psi \pi^+ \pi^-})$. The NR $\Lambda_b^0 \rightarrow J/\psi \pi^+ \pi^- pK^-$ component is described by the product of the Λ_b^0 signal template, an exponential function and a first-order polynomial function, $S_{\Lambda_b^0}(m_{J/\psi \pi^+ \pi^- pK^-}) \times E(m_{J/\psi \pi^+ \pi^-}) \times P_1(m_{J/\psi \pi^+ \pi^-})$, while the $\psi_{\pi\pi} pK^-$ component is parametrized as the product of the $\psi_{\pi\pi}$ signal template and an exponential function, $S_{\psi_{\pi\pi}}(m_{J/\psi \pi^+ \pi^-}) \times E(m_{J/\psi \pi^+ \pi^- pK^-})$. The combinatorial background is modelled by the function

$$f(m_{J/\psi \pi^+ \pi^- pK^-}, m_{J/\psi \pi^+ \pi^-}) = E(m_{J/\psi \pi^+ \pi^- pK^-}) \times \Phi_{3,5}(m_{J/\psi \pi^+ \pi^-}) \times P_3(m_{J/\psi \pi^+ \pi^- pK^-}, m_{J/\psi \pi^+ \pi^-}), \quad (4.1)$$

where $\Phi_{3,5}(m_{J/\psi \pi^+ \pi^-})$ is a three-body ($J/\psi \pi^+ \pi^-$) phase space function of the five-body Λ_b^0 decay [61], and P_3 is a two-dimensional positive third-order polynomial function in Bernstein form.

Projections of the two-dimensional fits to the $J/\psi \pi^+ \pi^- pK^-$ and $J/\psi \pi^+ \pi^-$ mass distributions for the intervals of $3.62 < m_{J/\psi \pi^+ \pi^-} < 3.72 \text{ GeV}/c^2$ and $3.80 < m_{J/\psi \pi^+ \pi^-} < 3.95 \text{ GeV}/c^2$ are shown in figure 1. The signal yields are determined to be 610 ± 30 and 55 ± 11 for the $\Lambda_b^0 \rightarrow \psi(2S)pK^-$ and $\Lambda_b^0 \rightarrow \chi_{c1}(3872)pK^-$ decay modes, respectively. The statistical significance of the observed $\Lambda_b^0 \rightarrow \chi_{c1}(3872)pK^-$ signal is estimated to be 7.2σ using Wilks' theorem [62] and confirmed by simulating a large number of pseudoexperiments according to the background distributions observed in data.

The background-subtracted pK^- mass spectrum [63] for the signal channel is shown in figure 2. The distribution exhibits a clear peak associated with the $\Lambda(1520)$ state. From this distribution the fraction of two-body $\Lambda_b^0 \rightarrow \chi_{c1}(3872)\Lambda(1520)$ decays is determined using an unbinned maximum-likelihood fit, which includes two components. The first component corresponds to the $\Lambda_b^0 \rightarrow \chi_{c1}(3872)\Lambda(1520)$ decay and is described with a relativistic P-wave Breit–Wigner function. The second component corresponds to the non-resonant decay $\Lambda_b^0 \rightarrow \chi_{c1}(3872)pK^-$ and is modelled by

$$B(m_{pK^-}) = \Phi_{2,3}(m_{pK^-}) \times P_1(m_{pK^-}), \quad (4.2)$$

where $\Phi_{2,3}(m_{pK^-})$ is a two-body (pK^-) phase space function of the three-body decay of the Λ_b^0 baryon and $P_1(m_{pK^-})$ a first-order polynomial function. The peak position and the natural width are constrained to the known values for the $\Lambda(1520)$ resonance [55]. The fraction of $\Lambda_b^0 \rightarrow \chi_{c1}(3872)\Lambda(1520)$ decays obtained from the fit is $(58 \pm 15)\%$, where the uncertainty is statistical only.

The ratio R defined in eq. (1.1) is obtained as

$$R = \frac{N_{\chi_{c1}(3872)pK^-}}{N_{\psi(2S)pK^-}} \times \frac{\varepsilon_{\psi(2S)pK^-}}{\varepsilon_{\chi_{c1}(3872)pK^-}}, \quad (4.3)$$

where N represents the measured yield and ε denotes the efficiency of the corresponding decay. The efficiency is defined as the product of the geometric acceptance and the detection, reconstruction, selection and trigger efficiencies. All efficiencies are determined using corrected simulated samples.

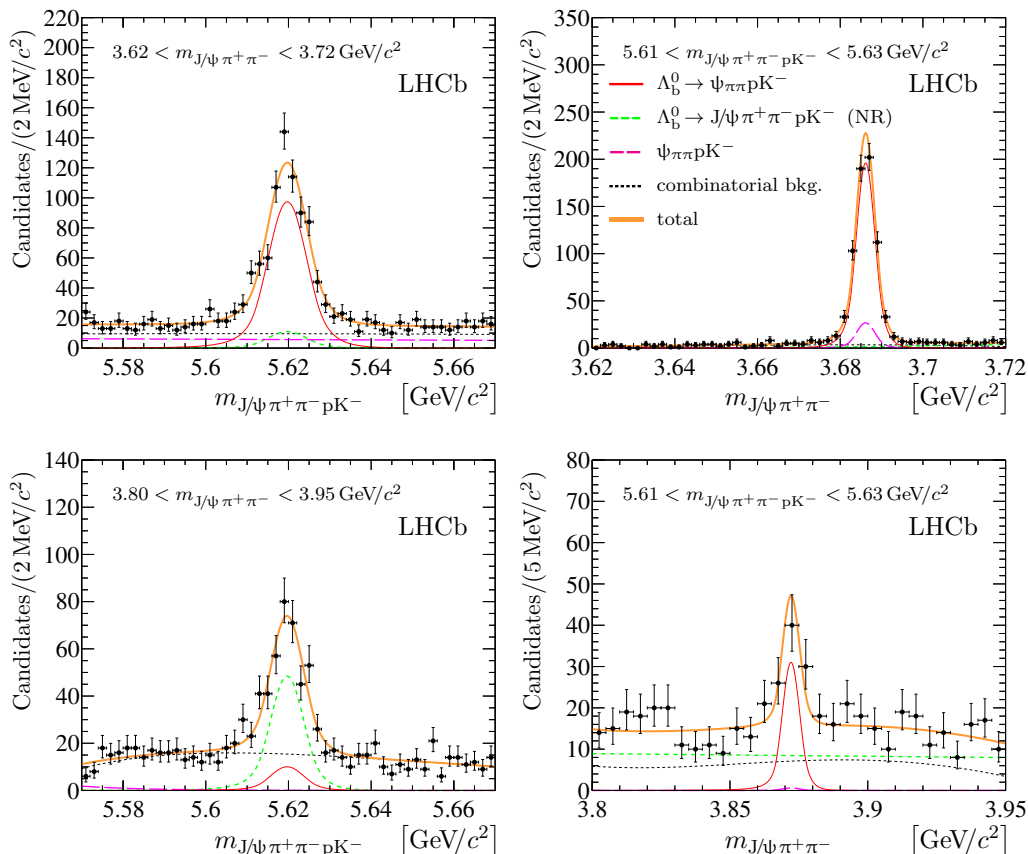


Figure 1. Projection of the two-dimensional distributions of (left) $J/\psi \pi^+ \pi^- pK^-$ and (right) $J/\psi \pi^+ \pi^-$ masses for the (top) $\Lambda_b^0 \rightarrow \psi(2S)pK^-$ and (bottom) $\Lambda_b^0 \rightarrow \chi_{c1}(3872)pK^-$ candidates.

The efficiencies are determined separately for each data-taking period and are combined according to the corresponding integrated luminosities [64] for each period and the known cross-section of b-hadron production in the LHCb acceptance [65–69]. The ratio of the efficiency of the normalization channel to that of the signal channel is determined to be

$$\frac{\epsilon_{\psi(2S)pK^-}}{\epsilon_{\chi_{c1}(3872)pK^-}} = 0.6065 \pm 0.0035, \quad (4.4)$$

where only the uncertainty that arises from the sizes of the simulated samples is given. Additional sources of uncertainty are discussed in the following section. The ratio of efficiencies differs from unity mainly due to different dipion mass spectra in the $\chi_{c1}(3872) \rightarrow J/\psi \pi^+ \pi^-$ and $\psi(2S) \rightarrow J/\psi \pi^+ \pi^-$ decays.

5 Systematic uncertainties

Since the signal and normalization decay channels have similar kinematics and topologies, a large part of systematic uncertainties cancel in the ratio R . The remaining contributions to the systematic uncertainty are listed in table 1 and discussed below.

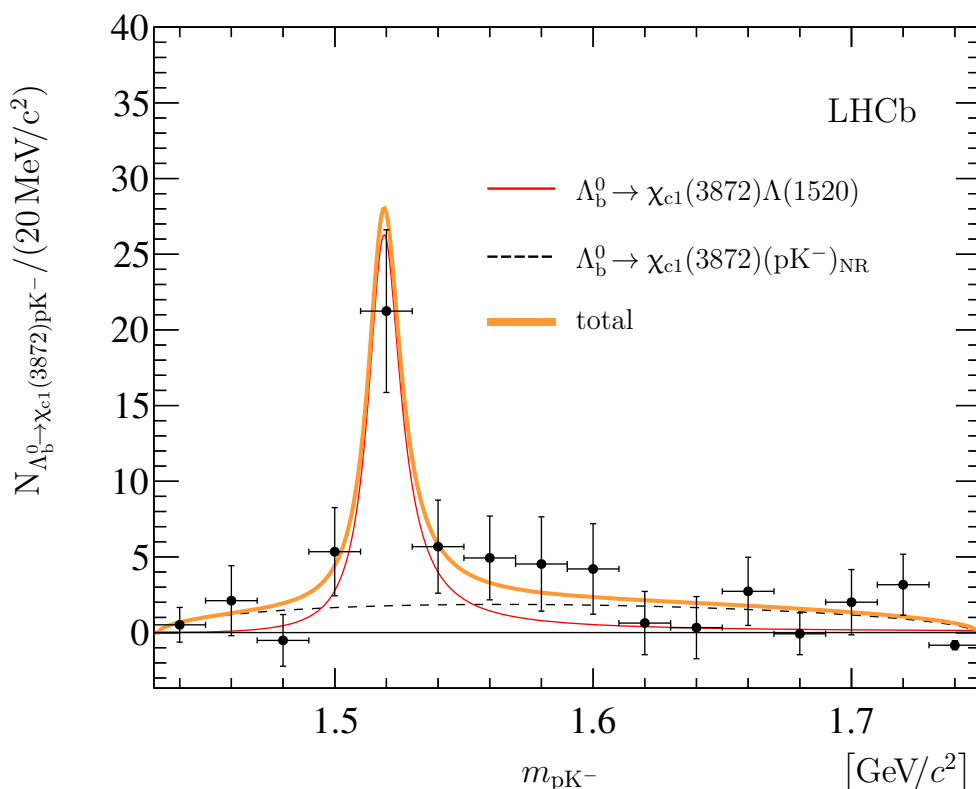


Figure 2. Background-subtracted mass distribution for the pK^- system in $\Lambda_b^0 \rightarrow \chi_{c1}(3872)pK^-$ decays with fit results in the range $1.43 < m_{pK^-} < 1.75 \text{ GeV}/c^2$ superimposed. The background subtraction is performed using the sPlot technique [63].

To estimate the systematic uncertainty related to the fit model, pseudoexperiments are generated according to the mass shapes obtained from the data fit. Each pseudoexperiment is then fitted with the baseline fit and alternative signal models and the ratio R is computed. A generalized Student’s t -distribution [70], an Apollonios function [71] and a modified Novosibirsk function [72] are used as alternative models for the signal component. The maximum relative bias found for the ratio R is 2%, which is assigned as a relative systematic uncertainty.

The simulated $\Lambda_b^0 \rightarrow \psi(2S)pK^-$ decays are corrected to reproduce the pK^- mass and $\cos \theta_{pK^-}$ distributions observed in data. The uncertainty associated with this correction procedure and related to the imperfect knowledge of the $\Lambda_b^0 \rightarrow \psi(2S)pK^-$ decay model is estimated by varying the reference kinematic m_{pK^-} and $\cos \theta_{pK^-}$ distributions within their uncertainties. It causes a negligible change of the efficiency $\epsilon_{\psi(2S)pK^-}$. A similar procedure applied to the $\Lambda_b^0 \rightarrow \chi_{c1}(3872)pK^-$ channel leads to a systematic uncertainty of 2% on the efficiency $\epsilon_{\chi_{c1}(3872)pK^-}$.

An additional uncertainty arises from the differences between data and simulation, in particular those affecting the efficiency for the reconstruction of charged-particle tracks. The small difference in the track-finding efficiency between data and simulation is corrected using data [58]. The uncertainties in these correction factors together with the uncertain-

Source	Uncertainty [%]
Fit model	2.0
Decay model of the $\Lambda_b^0 \rightarrow \chi_{c1}(3872)pK^-$ channel	2.0
Track reconstruction and hadron identification	0.4
Trigger	1.7
Selection criteria	1.0
Size of the simulated samples	0.6
Sum in quadrature	3.5

Table 1. Relative systematic uncertainties for the ratio of branching fractions.

ties in the hadron-identification efficiencies, related to the finite size of the calibration samples [43, 57], are propagated to the ratio of total efficiencies using pseudoexperiments. This results in a systematic uncertainty of 0.4% associated with track reconstruction and hadron identification.

To probe a possible mismodelling of the trigger efficiency, the ratio of efficiencies is calculated for various subsamples, matched to different trigger objects, namely dimuon vertex, high- p_T $\mu^+\mu^-$ pair, two-, three- and four-track secondary vertex, *etc.* The small difference of 1.7% in the ratio of trigger efficiencies between different subsamples is taken as systematic uncertainty due the trigger efficiency estimation. Another source of uncertainty is the potential disagreement between data and simulation in the estimation of efficiencies, due to effects not considered above. This is studied by varying the selection criteria in ranges that lead to as much as $\pm 20\%$ change in the measured signal yields. The stability is tested by comparing the efficiency-corrected yields within these variations. The resulting variations in the efficiency-corrected yields do not exceed 1%, which is taken as a corresponding systematic uncertainty [36]. The 0.6% relative uncertainty in the ratio of efficiencies from eq. (4.4) is assigned as a systematic uncertainty due to the finite size of the simulated samples.

The systematic uncertainty on the fraction of Λ_b^0 baryons decaying to the $\Lambda(1520)$ resonance is calculated by varying the parameters of the resonant and nonresonant components in the fit and found to be negligible with respect to the statistical uncertainty.

6 Results and summary

The decay $\Lambda_b^0 \rightarrow \chi_{c1}(3872)pK^-$ with $\chi_{c1}(3872) \rightarrow J/\psi \pi^+\pi^-$ is observed using data collected with the LHCb detector in proton-proton collisions corresponding to 1.0, 2.0 and 1.9 fb^{-1} of integrated luminosity at the centre-of-mass energies of 7, 8, and 13 TeV, respectively. The observed yield of $\Lambda_b^0 \rightarrow \chi_{c1}(3872)pK^-$ decays is 55 ± 11 with a statistical significance in excess of seven standard deviations. It is found that $(58 \pm 15)\%$ of the decays proceed via the two-body $\chi_{c1}(3872)\Lambda(1520)$ intermediate state.

Using the $\Lambda_b^0 \rightarrow \psi(2S)pK^-$, $\psi(2S) \rightarrow J/\psi \pi^+\pi^-$ decay as a normalization channel, the ratio of the branching fractions is measured to be

$$R = \frac{\mathcal{B}(\Lambda_b^0 \rightarrow \chi_{c1}(3872)pK^-)}{\mathcal{B}(\Lambda_b^0 \rightarrow \psi(2S)pK^-)} \times \frac{\mathcal{B}(\chi_{c1}(3872) \rightarrow J/\psi \pi^+\pi^-)}{\mathcal{B}(\psi(2S) \rightarrow J/\psi \pi^+\pi^-)} = (5.4 \pm 1.1 \pm 0.2) \times 10^{-2},$$

where the first uncertainty is statistical and the second is systematic.

Using the values of $\mathcal{B}(\Lambda_b^0 \rightarrow \psi(2S)pK^-)$ and $\mathcal{B}(\psi(2S) \rightarrow J/\psi \pi^+ \pi^-)$ taken from ref. [55] the product of branching fractions of interest is calculated to be

$$\mathcal{B}(\Lambda_b^0 \rightarrow \chi_{c1}(3872)pK^-) \times \mathcal{B}(\chi_{c1}(3872) \rightarrow J/\psi \pi^+ \pi^-) = (1.2 \pm 0.3 \pm 0.2) \times 10^{-6},$$

where the first uncertainty is statistical and the second is systematic, including the uncertainties on the branching fractions $\mathcal{B}(\Lambda_b^0 \rightarrow \psi(2S)pK^-)$ and $\mathcal{B}(\psi(2S) \rightarrow J/\psi \pi^+ \pi^-)$.

Acknowledgments

We express our gratitude to our colleagues in the CERN accelerator departments for the excellent performance of the LHC. We thank the technical and administrative staff at the LHCb institutes. We acknowledge support from CERN and from the national agencies: CAPES, CNPq, FAPERJ and FINEP (Brazil); MOST and NSFC (China); CNRS/IN2P3 (France); BMBF, DFG and MPG (Germany); INFN (Italy); NWO (Netherlands); MNiSW and NCN (Poland); MEN/IFA (Romania); MSHE (Russia); MinECo (Spain); SNSF and SER (Switzerland); NASU (Ukraine); STFC (United Kingdom); DOE NP and NSF (U.S.A.). We acknowledge the computing resources that are provided by CERN, IN2P3 (France), KIT and DESY (Germany), INFN (Italy), SURF (Netherlands), PIC (Spain), GridPP (United Kingdom), RRCKI and Yandex LLC (Russia), CSCS (Switzerland), IFIN-HH (Romania), CBPF (Brazil), PL-GRID (Poland) and OSC (U.S.A.). We are indebted to the communities behind the multiple open-source software packages on which we depend. Individual groups or members have received support from AvH Foundation (Germany); EPLANET, Marie Skłodowska-Curie Actions and ERC (European Union); ANR, Labex P2IO and OCEVU, and Région Auvergne-Rhône-Alpes (France); Key Research Program of Frontier Sciences of CAS, CAS PIFI, and the Thousand Talents Program (China); RFBR, RSF and Yandex LLC (Russia); GVA, XuntaGal and GENCAT (Spain); the Royal Society and the Leverhulme Trust (United Kingdom).

Open Access. This article is distributed under the terms of the Creative Commons Attribution License ([CC-BY 4.0](https://creativecommons.org/licenses/by/4.0/)), which permits any use, distribution and reproduction in any medium, provided the original author(s) and source are credited.

References

- [1] BELLE collaboration, *Observation of a narrow charmonium-like state in exclusive $B^\pm \rightarrow K^\pm \pi^+ \pi^- J/\psi$ decays*, *Phys. Rev. Lett.* **91** (2003) 262001 [[hep-ex/0309032](#)] [[INSPIRE](#)].
- [2] CDF collaboration, *Observation of the narrow state $X(3872) \rightarrow J/\psi \pi^+ \pi^-$ in $\bar{p}p$ collisions at $\sqrt{s} = 1.96$ TeV*, *Phys. Rev. Lett.* **93** (2004) 072001 [[hep-ex/0312021](#)] [[INSPIRE](#)].
- [3] D0 collaboration, *Observation and properties of the $X(3872)$ decaying to $J/\psi \pi^+ \pi^-$ in $p\bar{p}$ collisions at $\sqrt{s} = 1.96$ TeV*, *Phys. Rev. Lett.* **93** (2004) 162002 [[hep-ex/0405004](#)] [[INSPIRE](#)].
- [4] BABAR collaboration, *Study of the $B^- \rightarrow J/\psi K^- \pi^+ \pi^-$ decay and measurement of the $B^- \rightarrow X(3872)K^-$ branching fraction*, *Phys. Rev. D* **71** (2005) 071103 [[hep-ex/0406022](#)] [[INSPIRE](#)].

- [5] LHCb collaboration, *Observation of $X(3872)$ production in pp collisions at $\sqrt{s} = 7$ TeV*, *Eur. Phys. J. C* **72** (2012) 1972 [[arXiv:1112.5310](#)] [[INSPIRE](#)].
- [6] CMS collaboration, *Measurement of the $X(3872)$ production cross section via decays to $J/\psi\pi^+\pi^-$ in pp collisions at $\sqrt{s} = 7$ TeV*, *JHEP* **04** (2013) 154 [[arXiv:1302.3968](#)] [[INSPIRE](#)].
- [7] ATLAS collaboration, *Measurements of $\psi(2S)$ and $X(3872) \rightarrow J/\psi\pi^+\pi^-$ production in pp collisions at $\sqrt{s} = 8$ TeV with the ATLAS detector*, *JHEP* **01** (2017) 117 [[arXiv:1610.09303](#)] [[INSPIRE](#)].
- [8] CDF collaboration, *Precision measurement of the $X(3872)$ mass in $J/\psi\pi^+\pi^-$ decays*, *Phys. Rev. Lett.* **103** (2009) 152001 [[arXiv:0906.5218](#)] [[INSPIRE](#)].
- [9] CDF collaboration, *Measurement of the dipion mass spectrum in $X(3872) \rightarrow J/\psi\pi^+\pi^-$ decays*, *Phys. Rev. Lett.* **96** (2006) 102002 [[hep-ex/0512074](#)] [[INSPIRE](#)].
- [10] LHCb collaboration, *Quantum numbers of the $X(3872)$ state and orbital angular momentum in its $\rho^0 J\psi$ decay*, *Phys. Rev. D* **92** (2015) 011102 [[arXiv:1504.06339](#)] [[INSPIRE](#)].
- [11] S. Godfrey and S.L. Olsen, *The exotic XYZ charmonium-like mesons*, *Ann. Rev. Nucl. Part. Sci.* **58** (2008) 51 [[arXiv:0801.3867](#)].
- [12] W. Chen et al., *XYZ states*, *PoS(Hadron 2013)005* [[arXiv:1311.3763](#)] [[INSPIRE](#)].
- [13] N.N. Achasov and E.V. Rogozina, *$X(3872)$, $I^G(J^{PC}) = 0^+(1^{++})$, as the $\chi_{1c}(2P)$ charmonium*, *Mod. Phys. Lett. A* **30** (2015) 1550181 [[arXiv:1501.03583](#)] [[INSPIRE](#)].
- [14] N.N. Achasov, *Why $X(3872)$ is not a molecule*, *Phys. Part. Nucl.* **48** (2017) 839 [[INSPIRE](#)].
- [15] N.A. Törnqvist, *Isospin breaking of the narrow charmonium state of Belle at 3872 MeV as a deuson*, *Phys. Lett. B* **590** (2004) 209 [[hep-ph/0402237](#)] [[INSPIRE](#)].
- [16] E.S. Swanson, *Short range structure in the $X(3872)$* , *Phys. Lett. B* **588** (2004) 189 [[hep-ph/0311229](#)] [[INSPIRE](#)].
- [17] C.-Y. Wong, *Molecular states of heavy quark mesons*, *Phys. Rev. C* **69** (2004) 055202 [[hep-ph/0311088](#)] [[INSPIRE](#)].
- [18] L. Maiani, F. Piccinini, A.D. Polosa and V. Riquer, *Diquark-antidiquarks with hidden or open charm and the nature of $X(3872)$* , *Phys. Rev. D* **71** (2005) 014028 [[hep-ph/0412098](#)] [[INSPIRE](#)].
- [19] Z.-G. Wang and T. Huang, *Analysis of the $X(3872)$, $Z_c(3900)$ and $Z_c(3885)$ as axial-vector tetraquark states with QCD sum rules*, *Phys. Rev. D* **89** (2014) 054019 [[arXiv:1310.2422](#)] [[INSPIRE](#)].
- [20] B.A. Li, *Is $X(3872)$ a possible candidate of hybrid meson?*, *Phys. Lett. B* **605** (2005) 306 [[hep-ph/0410264](#)] [[INSPIRE](#)].
- [21] K.K. Seth, *An alternative interpretation of $X(3872)$* , *Phys. Lett. B* **612** (2005) 1 [[hep-ph/0411122](#)] [[INSPIRE](#)].
- [22] R.D. Matheus, F.S. Navarra, M. Nielsen and C.M. Zanetti, *QCD sum rules for the $X(3872)$ as a mixed molecule-charmonium state*, *Phys. Rev. D* **80** (2009) 056002 [[arXiv:0907.2683](#)] [[INSPIRE](#)].
- [23] W. Chen, H.-y. Jin, R.T. Kleiv, T.G. Steele, M. Wang and Q. Xu, *QCD sum-rule interpretation of $X(3872)$ with $J^{PC} = 1^{++}$ mixtures of hybrid charmonium and $\bar{D}D^*$ molecular currents*, *Phys. Rev. D* **88** (2013) 045027 [[arXiv:1305.0244](#)] [[INSPIRE](#)].

- [24] BABAR collaboration, *Evidence for $X(3872) \rightarrow \psi(2S)\gamma$ in $B^\pm \rightarrow X(3872)K^\pm$ decays and a study of $B \rightarrow c\bar{c}\gamma K$* , *Phys. Rev. Lett.* **102** (2009) 132001 [[arXiv:0809.0042](#)] [[INSPIRE](#)].
- [25] LHCb collaboration, *Evidence for the decay $X(3872) \rightarrow \psi(2S)\gamma$* , *Nucl. Phys. B* **886** (2014) 665 [[arXiv:1404.0275](#)] [[INSPIRE](#)].
- [26] BELLE collaboration, *Observation of $X(3872) \rightarrow J/\psi\gamma$ and search for $X(3872) \rightarrow \psi'\gamma$ in B decays*, *Phys. Rev. Lett.* **107** (2011) 091803 [[arXiv:1105.0177](#)] [[INSPIRE](#)].
- [27] E.S. Swanson, *Molecular interpretation of the $X(3872)$* , in the proceedings of the **32nd International Conference on High Energy Physics (ICHEP 2004)**, August 16–22, Beijing, China (2004), [hep-ph/0410284](#) [[INSPIRE](#)].
- [28] Y. Dong, A. Faessler, T. Gutsche and V.E. Lyubovitskij, *$J/\psi\gamma$ and $\psi(2S)\gamma$ decay modes of the $X(3872)$* , *J. Phys. G* **38** (2011) 015001 [[arXiv:0909.0380](#)] [[INSPIRE](#)].
- [29] J. Ferretti, G. Galatà and E. Santopinto, *Quark structure of the $X(3872)$ and $\chi_b(3P)$ resonances*, *Phys. Rev. D* **90** (2014) 054010 [[arXiv:1401.4431](#)] [[INSPIRE](#)].
- [30] LHCb collaboration, *Measurements of the $\Lambda_b^0 \rightarrow J/\psi\Lambda$ decay amplitudes and the Λ_b^0 polarisation in pp collisions at $\sqrt{s} = 7$ TeV*, *Phys. Lett. B* **724** (2013) 27 [[arXiv:1302.5578](#)] [[INSPIRE](#)].
- [31] LHCb collaboration, *Observation of $J/\psi p$ resonances consistent with pentaquark states in $\Lambda_b^0 \rightarrow J/\psi K^- p$ decays*, *Phys. Rev. Lett.* **115** (2015) 072001 [[arXiv:1507.03414](#)] [[INSPIRE](#)].
- [32] LHCb collaboration, *Observation of $\Lambda_b^0 \rightarrow \psi(2S)pK^-$ and $\Lambda_b^0 \rightarrow J/\psi\pi^+\pi^-pK^-$ decays and a measurement of the Λ_b^0 baryon mass*, *JHEP* **05** (2016) 132 [[arXiv:1603.06961](#)] [[INSPIRE](#)].
- [33] LHCb collaboration, *Evidence for exotic hadron contributions to $\Lambda_b^0 \rightarrow J/\psi p\pi^-$ decays*, *Phys. Rev. Lett.* **117** (2016) 082003 [*Phys. Rev. Lett.* **118** (2017) 119901] [[arXiv:1606.06999](#)] [[INSPIRE](#)].
- [34] LHCb collaboration, *Observation of the decays $\Lambda_b^0 \rightarrow \chi_{c1}pK^-$ and $\Lambda_b^0 \rightarrow \chi_{c2}pK^-$* , *Phys. Rev. Lett.* **119** (2017) 062001 [[arXiv:1704.07900](#)] [[INSPIRE](#)].
- [35] LHCb collaboration, *Measurement of the ratio of branching fractions of the decays $\Lambda_b^0 \rightarrow \psi(2S)\Lambda$ and $\Lambda_b^0 \rightarrow J/\psi\Lambda$* , *JHEP* **03** (2019) 126 [[arXiv:1902.02092](#)] [[INSPIRE](#)].
- [36] LHCb collaboration, *Observation of the decay $\Lambda_b^0 \rightarrow \psi(2S)p\pi^-$* , *JHEP* **08** (2018) 131 [[arXiv:1806.08084](#)] [[INSPIRE](#)].
- [37] CMS collaboration, *Measurement of the Λ_b polarization and angular parameters in $\Lambda_b \rightarrow J/\psi\Lambda$ decays from pp collisions at $\sqrt{s} = 7$ and 8 TeV*, *Phys. Rev. D* **97** (2018) 072010 [[arXiv:1802.04867](#)] [[INSPIRE](#)].
- [38] LHCb collaboration, *The LHCb detector at the LHC, 2008 JINST* **3** S08005 [[INSPIRE](#)].
- [39] LHCb collaboration, *LHCb detector performance*, *Int. J. Mod. Phys. A* **30** (2015) 1530022 [[arXiv:1412.6352](#)] [[INSPIRE](#)].
- [40] R. Aaij et al., *Performance of the LHCb Vertex Locator, 2014 JINST* **9** P09007 [[arXiv:1405.7808](#)] [[INSPIRE](#)].
- [41] R. Arink et al., *Performance of the LHCb Outer Tracker, 2014 JINST* **9** P01002 [[arXiv:1311.3893](#)] [[INSPIRE](#)].
- [42] P. d'Argent et al., *Improved performance of the LHCb Outer Tracker in LHC Run 2, 2017 JINST* **12** P11016 [[arXiv:1708.00819](#)] [[INSPIRE](#)].

- [43] M. Adinolfi et al., *Performance of the LHCb RICH detector at the LHC*, *Eur. Phys. J. C* **73** (2013) 2431 [[arXiv:1211.6759](#)] [[INSPIRE](#)].
- [44] A.A. Alves, Jr. et al., *Performance of the LHCb muon system*, *2013 JINST* **8** P02022 [[arXiv:1211.1346](#)] [[INSPIRE](#)].
- [45] R. Aaij et al., *The LHCb Trigger and its Performance in 2011*, *2013 JINST* **8** P04022 [[arXiv:1211.3055](#)] [[INSPIRE](#)].
- [46] T. Sjöstrand, S. Mrenna and P.Z. Skands, *A brief introduction to PYTHIA 8.1*, *Comput. Phys. Commun.* **178** (2008) 852 [[arXiv:0710.3820](#)] [[INSPIRE](#)].
- [47] I. Belyaev et al., *Handling of the generation of primary events in Gauss, the LHCb simulation framework*, *J. Phys. Conf. Ser.* **331** (2011) 032047 [[INSPIRE](#)].
- [48] D.J. Lange, *The EvtGen particle decay simulation package*, *Nucl. Instrum. Meth. A* **462** (2001) 152 [[INSPIRE](#)].
- [49] P. Golonka and Z. Was, *PHOTOS Monte Carlo: A Precision tool for QED corrections in Z and W decays*, *Eur. Phys. J. C* **45** (2006) 97 [[hep-ph/0506026](#)] [[INSPIRE](#)].
- [50] GEANT4 collaboration, *GEANT4 developments and applications*, *IEEE Trans. Nucl. Sci.* **53** (2006) 270.
- [51] GEANT4 collaboration, *GEANT4 — a simulation toolkit*, *Nucl. Instrum. Meth. A* **506** (2003) 250 [[INSPIRE](#)].
- [52] M. Clemencic et al., *The LHCb simulation application, Gauss: design, evolution and experience*, *J. Phys. Conf. Ser.* **331** (2011) 032023 [[INSPIRE](#)].
- [53] L. Breiman, J.H. Friedman, R.A. Olshen and C.J. Stone, *Classification and regression trees*, Wadsworth international group, Belmont, California U.S.A. (1984).
- [54] W.D. Hulsbergen, *Decay chain fitting with a Kalman filter*, *Nucl. Instrum. Meth. A* **552** (2005) 566 [[physics/0503191](#)] [[INSPIRE](#)].
- [55] PARTICLE DATA GROUP collaboration, *Review of particle physics*, *Phys. Rev. D* **98** (2018) 030001 [[INSPIRE](#)].
- [56] S. Geisser, *Predictive inference: an introduction*, Monographs on statistics and applied probability, Chapman & Hall, New York U.S.A. (1993).
- [57] R. Aaij et al., *Selection and processing of calibration samples to measure the particle identification performance of the LHCb experiment in Run 2*, *EPJ Tech. Instrum.* **6** (2019) 1 [[arXiv:1803.00824](#)] [[INSPIRE](#)].
- [58] LHCb collaboration, *Measurement of the track reconstruction efficiency at LHCb*, *2015 JINST* **10** P02007 [[arXiv:1408.1251](#)] [[INSPIRE](#)].
- [59] G. Punzi, *Sensitivity of searches for new signals and its optimization*, *eConf C* **030908** (2003) MODT002 [[physics/0308063](#)] [[INSPIRE](#)].
- [60] T. Skwarnicki, *A study of the radiative cascade transitions between the Υ' and Υ resonances*, *Ph.D. thesis*, Institute of Nuclear Physics, Krakow, Poland (1986).
- [61] E. Byckling and K. Kajantie, *Particle kinematics*, John Wiley & Sons Inc., U.S.A. (1973).
- [62] S.S. Wilks, *The large-sample distribution of the likelihood ratio for testing composite hypotheses*, *Annals Math. Statist.* **9** (1938) 60 [[INSPIRE](#)].

- [63] M. Pivk and F.R. Le Diberder, *SPlot: a statistical tool to unfold data distributions*, *Nucl. Instrum. Meth. A* **555** (2005) 356 [[physics/0402083](#)] [[INSPIRE](#)].
- [64] LHCb collaboration, *Precision luminosity measurements at LHCb, 2014 JINST* **9** P12005 [[arXiv:1410.0149](#)] [[INSPIRE](#)].
- [65] LHCb collaboration, *Measurement of $\sigma(pp \rightarrow b\bar{b}X)$ at $\sqrt{s} = 7$ TeV in the forward region*, *Phys. Lett. B* **694** (2010) 209 [[arXiv:1009.2731](#)] [[INSPIRE](#)].
- [66] LHCb collaboration, *Measurement of J/ψ production in pp collisions at $\sqrt{s} = 7$ TeV*, *Eur. Phys. J. C* **71** (2011) 1645 [[arXiv:1103.0423](#)] [[INSPIRE](#)].
- [67] LHCb collaboration, *Production of J/ψ and Υ mesons in pp collisions at $\sqrt{s} = 8$ TeV*, *JHEP* **06** (2013) 064 [[arXiv:1304.6977](#)] [[INSPIRE](#)].
- [68] LHCb collaboration, *Measurement of forward J/ψ production cross-sections in pp collisions at $\sqrt{s} = 13$ TeV*, *JHEP* **10** (2015) 172 [Erratum *ibid.* **1705** (2017) 063] [[arXiv:1509.00771](#)] [[INSPIRE](#)].
- [69] LHCb collaboration, *Measurement of the b -quark production cross-section in 7 and 13 TeV pp collisions*, *Phys. Rev. Lett.* **118** (2017) 052002 [Erratum *ibid.* **119** (2017) 169901] [[arXiv:1612.05140](#)] [[INSPIRE](#)].
- [70] S. Jackman, *Bayesian analysis for the social sciences*, John Wiley & Sons Inc., U.S.A. (2009).
- [71] D. Martínez Santos and F. Dupertuis, *Mass distributions marginalized over per-event errors*, *Nucl. Instrum. Meth. A* **764** (2014) 150 [[arXiv:1312.5000](#)] [[INSPIRE](#)].
- [72] BABAR collaboration, *Branching fraction measurements of the color-suppressed decays $\bar{B}^0 \rightarrow D^{(*)0}\pi^0$, $D^{(*)0}\eta$, $D^{(*)0}\omega$ and $D^{(*)0}\eta'$ and Measurement of the Polarization in the Decay $\bar{B}^0 \rightarrow D^{*0}\omega$* , *Phys. Rev. D* **84** (2011) 112007 [Erratum *ibid.* **D 87** (2013) 039901] [[arXiv:1107.5751](#)] [[INSPIRE](#)].

The LHCb collaboration

R. Aaij²⁹, C. Abellán Beteta⁴⁶, T. Ackernley⁵⁶, B. Adeva⁴³, M. Adinolfi⁵⁰, C.A. Aidala⁷⁸, S. Aiola²³, Z. Ajaltouni⁷, S. Akar⁶¹, P. Albicocco²⁰, J. Albrecht¹², F. Alessio⁴⁴, M. Alexander⁵⁵, A. Alfonso Albero⁴², G. Alkhazov³⁵, P. Alvarez Cartelle⁵⁷, A.A. Alves Jr⁴³, S. Amato², Y. Amhis⁹, L. An¹⁹, L. Anderlini¹⁹, G. Andreassi⁴⁵, M. Andreotti¹⁸, J.E. Andrews⁶², F. Archilli¹⁴, J. Arnau Romeu⁸, A. Artamonov⁴¹, M. Artuso⁶⁴, K. Arzymatov³⁹, E. Aslanides⁸, M. Atzeni⁴⁶, B. Audurier²⁴, S. Bachmann¹⁴, J.J. Back⁵², S. Baker⁵⁷, V. Balagura^{9,b}, W. Baldini^{18,44}, A. Baranov³⁹, R.J. Barlow⁵⁸, S. Barsuk⁹, W. Barter⁵⁷, M. Bartolini²¹, F. Baryshnikov⁷⁴, G. Bassi²⁶, V. Batozskaya³³, B. Batsukh⁶⁴, A. Battig¹², V. Battista⁴⁵, A. Bay⁴⁵, M. Becker¹², F. Bedeschi²⁶, I. Bediaga¹, A. Beiter⁶⁴, L.J. Bel²⁹, V. Belavin³⁹, S. Belin²⁴, N. Beliy⁴, V. Bellee⁴⁵, K. Belous⁴¹, I. Belyaev³⁶, G. Bencivenni²⁰, E. Ben-Haim¹⁰, S. Benson²⁹, S. Beranek¹¹, A. Berezhnoy³⁷, R. Bernet⁴⁶, D. Berninghoff¹⁴, E. Bertholet¹⁰, A. Bertolin²⁵, C. Betancourt⁴⁶, F. Betti^{17,e}, M.O. Bettler⁵¹, Ia. Bezshyiko⁴⁶, S. Bhasin⁵⁰, J. Bhom³¹, M.S. Bieker¹², S. Bifani⁴⁹, P. Billoir¹⁰, A. Birnkraut¹², A. Bizzeti^{19,u}, M. Bjørn⁵⁹, M.P. Blago⁴⁴, T. Blake⁵², F. Blanc⁴⁵, S. Blusk⁶⁴, D. Bobulska⁵⁵, V. Bocci²⁸, O. Boente Garcia⁴³, T. Boettcher⁶⁰, A. Boldyrev⁷⁵, A. Bondar^{40,y}, N. Bondar³⁵, S. Borghi^{58,44}, M. Borisyak³⁹, M. Borsato¹⁴, J.T. Borsuk³¹, M. Boubdir¹¹, T.J.V. Bowcock⁵⁶, C. Bozzi^{18,44}, S. Braun¹⁴, A. Brea Rodriguez⁴³, M. Brodski⁴⁴, J. Brodzicka³¹, A. Brossa Gonzalo⁵², D. Brundu^{24,44}, E. Buchanan⁵⁰, A. Buonaura⁴⁶, C. Burr⁴⁴, A. Bursche²⁴, J.S. Butter²⁹, J. Buytaert⁴⁴, W. Byczynski⁴⁴, S. Cadeddu²⁴, H. Cai⁶⁸, R. Calabrese^{18,g}, S. Cali²⁰, R. Calladine⁴⁹, M. Calvi^{22,i}, M. Calvo Gomez^{42,m}, A. Camboni^{42,m}, P. Campana²⁰, D.H. Campora Perez⁴⁴, L. Capriotti^{17,e}, A. Carbone^{17,e}, G. Carboni²⁷, R. Cardinale²¹, A. Cardini²⁴, P. Carniti^{22,i}, K. Carvalho Akiba², A. Casais Vidal⁴³, G. Casse⁵⁶, M. Cattaneo⁴⁴, G. Cavallero²¹, R. Cenci^{26,p}, J. Cerasoli⁸, M.G. Chapman⁵⁰, M. Charles^{10,44}, Ph. Charpentier⁴⁴, G. Chatzikonstantinidis⁴⁹, M. Chefdeville⁶, V. Chekalina³⁹, C. Chen³, S. Chen²⁴, A. Chernov³¹, S.-G. Chitic⁴⁴, V. Chobanova⁴³, M. Chrzaszcz⁴⁴, A. Chubykin³⁵, P. Ciambone²⁰, M.F. Cicala⁵², X. Cid Vidal⁴³, G. Ciezarek⁴⁴, F. Cindolo¹⁷, P.E.L. Clarke⁵⁴, M. Clemencic⁴⁴, H.V. Cliff⁵¹, J. Closier⁴⁴, J.L. Cobbedick⁵⁸, V. Coco⁴⁴, J.A.B. Coelho⁹, J. Cogan⁸, E. Cogneras⁷, L. Cojocariu³⁴, P. Collins⁴⁴, T. Colombo⁴⁴, A. Comerma-Montells¹⁴, A. Contu²⁴, N. Cooke⁴⁹, G. Coombs⁵⁵, S. Coquereau⁴², G. Corti⁴⁴, C.M. Costa Sobral⁵², B. Couturier⁴⁴, G.A. Cowan⁵⁴, D.C. Craik⁶⁰, A. Crocombe⁵², M. Cruz Torres¹, R. Currie⁵⁴, C.L. Da Silva⁶³, E. Dall'Occo²⁹, J. Dalseno^{43,w}, C. D'Ambrosio⁴⁴, A. Danilina³⁶, P. d'Argent¹⁴, A. Davis⁵⁸, O. De Aguiar Francisco⁴⁴, K. De Bruyn⁴⁴, S. De Capua⁵⁸, M. De Cian⁴⁵, J.M. De Miranda¹, L. De Paula², M. De Serio^{16,d}, P. De Simone²⁰, J.A. de Vries²⁹, C.T. Dean⁶³, W. Dean⁷⁸, D. Decamp⁶, L. Del Buono¹⁰, B. Delaney⁵¹, H.-P. Dembinski¹³, M. Demmer¹², A. Dendek³², V. Denysenko⁴⁶, D. Derkach⁷⁵, O. Deschamps⁷, F. Desse⁹, F. Dettori²⁴, B. Dey⁶⁹, A. Di Canto⁴⁴, P. Di Nezza²⁰, S. Didenko⁷⁴, H. Dijkstra⁴⁴, F. Dordei²⁴, M. Dorigo^{26,z}, A.C. dos Reis¹, A. Dosil Suárez⁴³, L. Douglas⁵⁵, A. Dovbnya⁴⁷, K. Dreimanis⁵⁶, M.W. Dudek³¹, L. Dufour⁴⁴, G. Dujany¹⁰, P. Durante⁴⁴, J.M. Durham⁶³, D. Dutta⁵⁸, R. Dzhelyadin^{41,†}, M. Dziewiecki¹⁴, A. Dziurda³¹, A. Dzyuba³⁵, S. Easo⁵³, U. Egede⁵⁷, V. Egorychev³⁶, S. Eidelman^{40,y}, S. Eisenhardt⁵⁴, U. Eitschberger¹², R. Ekelhof¹², S. Ek-In⁴⁵, L. Eklund⁵⁵, S. Ely⁶⁴, A. Ene³⁴, S. Escher¹¹, S. Esen²⁹, T. Evans⁶¹, A. Falabella¹⁷, J. Fan³, N. Farley⁴⁹, S. Farry⁵⁶, D. Fazzini⁹, M. Féo⁴⁴, P. Fernandez Declara⁴⁴, A. Fernandez Prieto⁴³, F. Ferrari^{17,e}, L. Ferreira Lopes⁴⁵, F. Ferreira Rodrigues², S. Ferreres Sole²⁹, M. Ferro-Luzzi⁴⁴, S. Filippov³⁸, R.A. Fini¹⁶, M. Fiorini^{18,g}, M. Firlej³², K.M. Fischer⁵⁹, C. Fitzpatrick⁴⁴, T. Fiutowski³², F. Fleuret^{9,b}, M. Fontana⁴⁴, F. Fontanelli^{21,h}, R. Forty⁴⁴, V. Franco Lima⁵⁶, M. Franco Sevilla⁶², M. Frank⁴⁴, C. Frei⁴⁴, D.A. Friday⁵⁵, J. Fu^{23,q}, W. Funk⁴⁴, E. Gabriel⁵⁴, A. Gallas Torreira⁴³, D. Galli^{17,e}, S. Gallorini²⁵,

S. Gambetta⁵⁴, Y. Gan³, M. Gandelman², P. Gandini²³, Y. Gao³, L.M. Garcia Martin⁷⁷,
 J. García Pardiñas⁴⁶, B. Garcia Plana⁴³, F.A. Garcia Rosales⁹, J. Garra Tico⁵¹, L. Garrido⁴²,
 D. Gascon⁴², C. Gaspar⁴⁴, G. Gazzoni⁷, D. Gerick¹⁴, E. Gersabeck⁵⁸, M. Gersabeck⁵⁸,
 T. Gershon⁵², D. Gerstel⁸, Ph. Ghez⁶, V. Gibson⁵¹, A. Gioventù⁴³, O.G. Girard⁴⁵,
 P. Gironella Gironell⁴², L. Giubega³⁴, K. Gizdov⁵⁴, V.V. Gligorov¹⁰, C. Göbel⁶⁶, D. Golubkov³⁶,
 A. Golutvin^{57,74}, A. Gomes^{1,a}, I.V. Gorelov³⁷, C. Gotti^{22,i}, E. Govorkova²⁹, J.P. Grabowski¹⁴,
 R. Graciani Diaz⁴², T. Grammatico¹⁰, L.A. Granado Cardoso⁴⁴, E. Graugés⁴², E. Graverini⁴⁵,
 G. Graziani¹⁹, A. Grecu³⁴, R. Greim²⁹, P. Griffith²⁴, L. Grillo⁵⁸, L. Gruber⁴⁴,
 B.R. Gruberg Cazon⁵⁹, C. Gu³, E. Gushchin³⁸, A. Guth¹¹, Yu. Guz^{41,44}, T. Gys⁴⁴,
 T. Hadavizadeh⁵⁹, C. Hadjivasiliou⁷, G. Haefeli⁴⁵, C. Haen⁴⁴, S.C. Haines⁵¹, P.M. Hamilton⁶²,
 Q. Han⁶⁹, X. Han¹⁴, T.H. Hancock⁵⁹, S. Hansmann-Menzemer¹⁴, N. Harnew⁵⁹, T. Harrison⁵⁶,
 C. Hasse⁴⁴, M. Hatch⁴⁴, J. He⁴, M. Hecker⁵⁷, K. Heijhoff²⁹, K. Heinicke¹², A. Heister¹²,
 K. Hennessy⁵⁶, L. Henry⁷⁷, M. Heß⁷¹, J. Heuel¹¹, A. Hicheur⁶⁵, R. Hidalgo Charman⁵⁸, D. Hill⁵⁹,
 M. Hilton⁵⁸, P.H. Hopchev⁴⁵, J. Hu¹⁴, W. Hu⁶⁹, W. Huang⁴, Z.C. Huard⁶¹, W. Hulsbergen²⁹,
 T. Humair⁵⁷, R.J. Hunter⁵², M. Hushchyn⁷⁵, D. Hutchcroft⁵⁶, D. Hynds²⁹, P. Ibis¹², M. Idzik³²,
 P. Ilten⁴⁹, A. Inglese³⁵, A. Inyakin⁴¹, K. Ivshin³⁵, R. Jacobsson⁴⁴, S. Jakobsen⁴⁴, J. Jalocha⁵⁹,
 E. Jans²⁹, B.K. Jashal⁷⁷, A. Jawahery⁶², F. Jiang³, M. John⁵⁹, D. Johnson⁴⁴, C.R. Jones⁵¹,
 B. Jost⁴⁴, N. Jurik⁵⁹, S. Kandybei⁴⁷, M. Karacson⁴⁴, J.M. Kariuki⁵⁰, S. Karodia⁵⁵, N. Kazeev⁷⁵,
 M. Kecke¹⁴, F. Keizer⁵¹, M. Kelsey⁶⁴, M. Kenzie⁵¹, T. Ketel³⁰, B. Khanji⁴⁴, A. Kharisova⁷⁶,
 C. Khurewathanakul⁴⁵, K.E. Kim⁶⁴, T. Kirn¹¹, V.S. Kirsebom⁴⁵, S. Klaver²⁰, K. Klimaszewski³³,
 P. Kodassery Padmalayammadam³¹, S. Koliiev⁴⁸, A. Kondybayeva⁷⁴, A. Konoplyannikov³⁶,
 P. Kopciewicz³², R. Kopecna¹⁴, P. Koppenburg²⁹, I. Kostiuik^{29,48}, O. Kot⁴⁸, S. Kotriakhova³⁵,
 M. Kozeiha⁷, L. Kravchuk³⁸, R.D. Krawczyk⁴⁴, M. Kreps⁵², F. Kress⁵⁷, S. Kretzschmar¹¹,
 P. Krokovny^{40,y}, W. Krupa³², W. Krzemien³³, W. Kuczewicz^{31,l}, M. Kucharczyk³¹,
 V. Kudryavtsev^{40,y}, H.S. Kuindersma²⁹, G.J. Kunde⁶³, A.K. Kuonen⁴⁵, T. Kvaratskheliya³⁶,
 D. Lacarrere⁴⁴, G. Lafferty⁵⁸, A. Lai²⁴, D. Lancierini⁴⁶, J.J. Lane⁵⁸, G. Lanfranchi²⁰,
 C. Langenbruch¹¹, T. Latham⁵², F. Lazzari^{26,v}, C. Lazzeroni⁴⁹, R. Le Gac⁸, R. Lefèvre⁷,
 A. Leflat³⁷, F. Lemaitre⁴⁴, O. Leroy⁸, T. Lesiak³¹, B. Leverington¹⁴, H. Li⁶⁷, P.-R. Li^{4,ac}, X. Li⁶³,
 Y. Li⁵, Z. Li⁶⁴, X. Liang⁶⁴, T. Likhomanenko⁷³, R. Lindner⁴⁴, F. Lionetto⁴⁶, V. Lisovskyi⁹,
 G. Liu⁶⁷, X. Liu³, D. Loh⁵², A. Loi²⁴, J. Lomba Castro⁴³, I. Longstaff⁵⁵, J.H. Lopes²,
 G. Loustau⁴⁶, G.H. Lovell⁵¹, D. Lucchesi^{25,o}, M. Lucio Martinez²⁹, Y. Luo³, A. Lupato²⁵,
 E. Luppi^{18,g}, O. Lupton⁵², A. Lusiani²⁶, X. Lyu⁴, S. Maccolini^{17,e}, F. Machefert⁹, F. Maciuc³⁴,
 V. Macko⁴⁵, P. Mackowiak¹², S. Maddrell-Mander⁵⁰, L.R. Madhan Mohan⁵⁰, O. Maev^{35,44},
 A. Maevskiy⁷⁵, K. Maguire⁵⁸, D. Maisuzenko³⁵, M.W. Majewski³², S. Malde⁵⁹, B. Malecki⁴⁴,
 A. Malinin⁷³, T. Maltsev^{40,y}, H. Malygina¹⁴, G. Manca^{24,f}, G. Mancinelli⁸, D. Manuzzi^{17,e},
 D. Marangotto^{23,q}, J. Maratas^{7,x}, J.F. Marchand⁶, U. Marconi¹⁷, S. Mariani¹⁹, C. Marin Benito⁹,
 M. Marinangeli⁴⁵, P. Marino⁴⁵, J. Marks¹⁴, P.J. Marshall⁵⁶, G. Martellotti²⁸, L. Martinazzoli⁴⁴,
 M. Martinelli^{44,22,i}, D. Martinez Santos⁴³, F. Martinez Vidal⁷⁷, A. Massafferri¹, M. Materok¹¹,
 R. Matev⁴⁴, A. Mathad⁴⁶, Z. Mathe⁴⁴, V. Matiunin³⁶, C. Matteuzzi²², K.R. Mattioli⁷⁸,
 A. Mauri⁴⁶, E. Maurice^{9,b}, M. McCann^{57,44}, L. McConnell¹⁵, A. McNab⁵⁸, R. McNulty¹⁵,
 J.V. Mead⁵⁶, B. Meadows⁶¹, C. Meaux⁸, N. Meinert⁷¹, D. Melnychuk³³, S. Meloni^{22,i}, M. Merk²⁹,
 A. Merli^{23,q}, E. Michielin²⁵, D.A. Milanese⁷⁰, E. Millard⁵², M.-N. Minard⁶, O. Mineev³⁶,
 L. Minzoni^{18,g}, S.E. Mitchell⁵⁴, B. Mitreska⁵⁸, D.S. Mitzel⁴⁴, A. Mödden¹², A. Mogini¹⁰,
 R.D. Moise⁵⁷, T. Mombächer¹², I.A. Monroy⁷⁰, S. Monteil⁷, M. Morandin²⁵, G. Morello²⁰,
 M.J. Morello^{26,t}, J. Moron³², A.B. Morris⁸, A.G. Morris⁵², R. Mountain⁶⁴, H. Mu³, F. Muheim⁵⁴,
 M. Mukherjee⁶⁹, M. Mulder²⁹, D. Müller⁴⁴, J. Müller¹², K. Müller⁴⁶, V. Müller¹², C.H. Murphy⁵⁹,
 D. Murray⁵⁸, P. Naik⁵⁰, T. Nakada⁴⁵, R. Nandakumar⁵³, A. Nandi⁵⁹, T. Nanut⁴⁵, I. Nasteva²,
 M. Needham⁵⁴, N. Neri^{23,q}, S. Neubert¹⁴, N. Neufeld⁴⁴, R. Newcombe⁵⁷, T.D. Nguyen⁴⁵,

C. Nguyen-Mau^{45,n}, E.M. Niel⁹, S. Nieswand¹¹, N. Nikitin³⁷, N.S. Nolte⁴⁴,
A. Oblakowska-Mucha³², V. Obraztsov⁴¹, S. Ogilvy⁵⁵, D.P. O’Hanlon¹⁷, R. Oldeman^{24,f},
C.J.G. Onderwater⁷², J. D. Osborn⁷⁸, A. Ossowska³¹, J.M. Otalora Goicochea²,
T. Ovsianikova³⁶, P. Owen⁴⁶, A. Oyanguren⁷⁷, P.R. Pais⁴⁵, T. Pajero^{26,t}, A. Palano¹⁶,
M. Palutan²⁰, G. Panshin⁷⁶, A. Papanestis⁵³, M. Pappagallo⁵⁴, L.L. Pappalardo^{18,g}, W. Parker⁶²,
C. Parkes^{58,44}, G. Passaleva^{19,44}, A. Pastore¹⁶, M. Patel⁵⁷, C. Patrignani^{17,e}, A. Pearce⁴⁴,
A. Pellegrino²⁹, G. Penso²⁸, M. Pepe Altarelli⁴⁴, S. Perazzini¹⁷, D. Pereima³⁶, P. Perret⁷,
L. Pescatore⁴⁵, K. Petridis⁵⁰, A. Petrolini^{21,h}, A. Petrov⁷³, S. Petrucci⁵⁴, M. Petruzzo^{23,q},
B. Pietrzyk⁶, G. Pietrzyk⁴⁵, M. Pikies³¹, M. Pili⁵⁹, D. Pinci²⁸, J. Pinzino⁴⁴, F. Pisani⁴⁴,
A. Piucci¹⁴, V. Placinta³⁴, S. Playfer⁵⁴, J. Plews⁴⁹, M. Plo Casasus⁴³, F. Polci¹⁰, M. Poli Lener²⁰,
M. Poliakov⁶⁴, A. Poluektov⁸, N. Polukhina^{74,c}, I. Polyakov⁶⁴, E. Polcarpo², G.J. Pomery⁵⁰,
S. Ponce⁴⁴, A. Popov⁴¹, D. Popov⁴⁹, S. Poslavskii⁴¹, L. Promberger⁴⁴, C. Prouve⁴³, V. Pugatch⁴⁸,
A. Puig Navarro⁴⁶, H. Pullen⁵⁹, G. Punzi^{26,p}, W. Qian⁴, J. Qin⁴, R. Quagliani¹⁰, B. Quintana⁷,
N.V. Raab¹⁵, B. Rachwal³², J.H. Rademacker⁵⁰, M. Rama²⁶, M. Ramos Pernas⁴³, M.S. Rangel²,
F. Ratnikov^{39,75}, G. Raven³⁰, M. Ravonel Salzgeber⁴⁴, M. Reboud⁶, F. Redi⁴⁵, S. Reichert¹²,
F. Reiss¹⁰, C. Remon Alepuz⁷⁷, Z. Ren³, V. Renaudin⁵⁹, S. Ricciardi⁵³, S. Richards⁵⁰,
K. Rinnert⁵⁶, P. Robbe⁹, A. Robert¹⁰, A.B. Rodrigues⁴⁵, E. Rodrigues⁶¹, J.A. Rodriguez Lopez⁷⁰,
M. Roehrken⁴⁴, S. Roiser⁴⁴, A. Rollings⁵⁹, V. Romanovskiy⁴¹, M. Romero Lamas⁴³,
A. Romero Vidal⁴³, J.D. Roth⁷⁸, M. Rotondo²⁰, M.S. Rudolph⁶⁴, T. Ruf⁴⁴, J. Ruiz Vidal⁷⁷,
J. Ryzka³², J.J. Saborido Silva⁴³, N. Sagidova³⁵, B. Saitta^{24,f}, C. Sanchez Gras²⁹,
C. Sanchez Mayordomo⁷⁷, B. Sanmartin Sedes⁴³, R. Santacesaria²⁸, C. Santamarina Rios⁴³,
P. Santangelo²⁰, M. Santimaria^{20,44}, E. Santovetti^{27,j}, G. Sarpis⁵⁸, A. Sarti^{20,k}, C. Satriano^{28,s},
A. Satta²⁷, M. Saur⁴, D. Savrina^{36,37}, L.G. Scantlebury Smead⁵⁹, S. Schael¹¹, M. Schellenberg¹²,
M. Schiller⁵⁵, H. Schindler⁴⁴, M. Schmelling¹³, T. Schmelzer¹², B. Schmidt⁴⁴, O. Schneider⁴⁵,
A. Schopper⁴⁴, H.F. Schreiner⁶¹, M. Schubiger²⁹, S. Schulte⁴⁵, M.H. Schune⁹, R. Schwemmer⁴⁴,
B. Sciascia²⁰, A. Sciubba^{28,k}, A. Semennikov³⁶, A. Sergi^{49,44}, N. Serra⁴⁶, J. Serrano⁸, L. Sestini²⁵,
A. Seuthe¹², P. Seyfert⁴⁴, M. Shapkin⁴¹, T. Shears⁵⁶, L. Shekhtman^{40,y}, V. Shevchenko^{73,74},
E. Shmanin⁷⁴, J.D. Shupperd⁶⁴, B.G. Siddi¹⁸, R. Silva Coutinho⁴⁶, L. Silva de Oliveira²,
G. Simi^{25,o}, S. Simone^{16,d}, I. Skiba¹⁸, N. Skidmore¹⁴, T. Skwarnicki⁶⁴, M.W. Slater⁴⁹,
J.G. Smeaton⁵¹, E. Smith¹¹, I.T. Smith⁵⁴, M. Smith⁵⁷, M. Soares¹⁷, I. Soares Lavra¹,
M.D. Sokoloff⁶¹, F.J.P. Soler⁵⁵, B. Souza De Paula², B. Spaan¹², E. Spadaro Norella^{23,q},
P. Spradlin⁵⁵, F. Stagni⁴⁴, M. Stahl⁶¹, S. Stahl⁴⁴, P. Stefko⁴⁵, S. Stefkova⁵⁷, O. Steinkamp⁴⁶,
S. Stemmler¹⁴, O. Stenyakin⁴¹, M. Stepanova³⁵, H. Stevens¹², A. Stocchi⁹, S. Stone⁶⁴, S. Stracka²⁶,
M.E. Stramaglia⁴⁵, M. Straticiu³⁴, U. Straumann⁴⁶, S. Strovkov⁷⁶, J. Sun³, L. Sun⁶⁸, Y. Sun⁶²,
K. Swientek³², A. Szabelski³³, T. Szumlak³², M. Szymanski⁴, S. Taneja⁵⁸, Z. Tang³,
T. Tekampe¹², G. Tellarini¹⁸, F. Teubert⁴⁴, E. Thomas⁴⁴, K.A. Thomson⁵⁶, M.J. Tilley⁵⁷,
V. Tisserand⁷, S. T’Jampens⁶, M. Tobin⁵, S. Tol⁴⁴, L. Tomassetti^{18,g}, D. Tonelli²⁶, D.Y. Tou¹⁰,
E. Tournefier⁶, M. Traill⁵⁵, M.T. Tran⁴⁵, A. Trisovic⁵¹, A. Tsaregorodtsev⁸, G. Tuci^{26,44,p},
A. Tully⁵¹, N. Tuning²⁹, A. Ukleja³³, A. Usachov⁹, A. Ustyuzhanin^{39,75}, U. Uwer¹⁴, A. Vagner⁷⁶,
V. Vagnoni¹⁷, A. Valassi⁴⁴, S. Valat⁴⁴, G. Valenti¹⁷, M. van Beuzekom²⁹, H. Van Hecke⁶³,
E. van Herwijnen⁴⁴, C.B. Van Hulse¹⁵, J. van Tilburg²⁹, M. van Veghel⁷², R. Vazquez Gomez⁴⁴,
P. Vazquez Regueiro⁴³, C. Vázquez Sierra²⁹, S. Vecchi¹⁸, J.J. Velthuis⁵⁰, M. Veltri^{19,r},
A. Venkateswaran⁶⁴, M. Vernet⁷, M. Veronesi²⁹, M. Vesterinen⁵², J.V. Viana Barbosa⁴⁴,
D. Vieira⁴, M. Vieites Diaz⁴⁵, H. Viemann⁷¹, X. Vilasis-Cardona^{42,m}, A. Vitkovskiy²⁹,
V. Volkov³⁷, A. Vollhardt⁴⁶, D. Vom Bruch¹⁰, B. Voneki⁴⁴, A. Vorobyev³⁵, V. Vorobyev^{40,y},
N. Voropaev³⁵, R. Waldi⁷¹, J. Walsh²⁶, J. Wang³, J. Wang⁵, M. Wang³, Y. Wang⁶⁹, Z. Wang⁴⁶,
D.R. Ward⁵¹, H.M. Wark⁵⁶, N.K. Watson⁴⁹, D. Websdale⁵⁷, A. Weiden⁴⁶, C. Weisser⁶⁰,
B.D.C. Westhenry⁵⁰, D.J. White⁵⁸, M. Whitehead¹¹, D. Wiedner¹⁹, G. Wilkinson⁵⁹,

M. Wilkinson⁶⁴, I. Williams⁵¹, M. Williams⁶⁰, M.R.J. Williams⁵⁸, T. Williams⁴⁹, F.F. Wilson⁵³,
M. Winn⁹, W. Wislicki³³, M. Witek³¹, G. Wormser⁹, S.A. Wotton⁵¹, H. Wu⁶⁴, K. Wyllie⁴⁴,
Z. Xiang⁴, D. Xiao⁶⁹, Y. Xie⁶⁹, H. Xing⁶⁷, A. Xu³, L. Xu³, M. Xu⁶⁹, Q. Xu⁴, Z. Xu⁶, Z. Xu³,
Z. Yang³, Z. Yang⁶², Y. Yao⁶⁴, L.E. Yeomans⁵⁶, H. Yin⁶⁹, J. Yu^{69,ab}, X. Yuan⁶⁴,
O. Yushchenko⁴¹, K.A. Zarebski⁴⁹, M. Zavertyaev^{13,c}, M. Zdybal³¹, M. Zeng³, D. Zhang⁶⁹,
L. Zhang³, S. Zhang³, W.C. Zhang^{3,aa}, Y. Zhang⁴⁴, A. Zhelezov¹⁴, Y. Zheng⁴, X. Zhou⁴,
Y. Zhou⁴, X. Zhu³, V. Zhukov^{11,37}, J.B. Zonneveld⁵⁴, S. Zucchelli^{17,e}

- ¹ *Centro Brasileiro de Pesquisas Físicas (CBPF), Rio de Janeiro, Brazil*
- ² *Universidade Federal do Rio de Janeiro (UFRJ), Rio de Janeiro, Brazil*
- ³ *Center for High Energy Physics, Tsinghua University, Beijing, China*
- ⁴ *University of Chinese Academy of Sciences, Beijing, China*
- ⁵ *Institute Of High Energy Physics (ihep), Beijing, China*
- ⁶ *Univ. Grenoble Alpes, Univ. Savoie Mont Blanc, CNRS, IN2P3-LAPP, Annecy, France*
- ⁷ *Université Clermont Auvergne, CNRS/IN2P3, LPC, Clermont-Ferrand, France*
- ⁸ *Aix Marseille Univ, CNRS/IN2P3, CPPM, Marseille, France*
- ⁹ *LAL, Univ. Paris-Sud, CNRS/IN2P3, Université Paris-Saclay, Orsay, France*
- ¹⁰ *LPNHE, Sorbonne Université, Paris Diderot Sorbonne Paris Cité, CNRS/IN2P3, Paris, France*
- ¹¹ *I. Physikalisches Institut, RWTH Aachen University, Aachen, Germany*
- ¹² *Fakultät Physik, Technische Universität Dortmund, Dortmund, Germany*
- ¹³ *Max-Planck-Institut für Kernphysik (MPIK), Heidelberg, Germany*
- ¹⁴ *Physikalisches Institut, Ruprecht-Karls-Universität Heidelberg, Heidelberg, Germany*
- ¹⁵ *School of Physics, University College Dublin, Dublin, Ireland*
- ¹⁶ *INFN Sezione di Bari, Bari, Italy*
- ¹⁷ *INFN Sezione di Bologna, Bologna, Italy*
- ¹⁸ *INFN Sezione di Ferrara, Ferrara, Italy*
- ¹⁹ *INFN Sezione di Firenze, Firenze, Italy*
- ²⁰ *INFN Laboratori Nazionali di Frascati, Frascati, Italy*
- ²¹ *INFN Sezione di Genova, Genova, Italy*
- ²² *INFN Sezione di Milano-Bicocca, Milano, Italy*
- ²³ *INFN Sezione di Milano, Milano, Italy*
- ²⁴ *INFN Sezione di Cagliari, Monserrato, Italy*
- ²⁵ *INFN Sezione di Padova, Padova, Italy*
- ²⁶ *INFN Sezione di Pisa, Pisa, Italy*
- ²⁷ *INFN Sezione di Roma Tor Vergata, Roma, Italy*
- ²⁸ *INFN Sezione di Roma La Sapienza, Roma, Italy*
- ²⁹ *Nikhef National Institute for Subatomic Physics, Amsterdam, Netherlands*
- ³⁰ *Nikhef National Institute for Subatomic Physics and VU University Amsterdam, Amsterdam, Netherlands*
- ³¹ *Henryk Niewodniczanski Institute of Nuclear Physics Polish Academy of Sciences, Kraków, Poland*
- ³² *AGH - University of Science and Technology, Faculty of Physics and Applied Computer Science, Kraków, Poland*
- ³³ *National Center for Nuclear Research (NCBJ), Warsaw, Poland*
- ³⁴ *Horia Hulubei National Institute of Physics and Nuclear Engineering, Bucharest-Magurele, Romania*
- ³⁵ *Petersburg Nuclear Physics Institute NRC Kurchatov Institute (PNPI NRC KI), Gatchina, Russia*
- ³⁶ *Institute of Theoretical and Experimental Physics NRC Kurchatov Institute (ITEP NRC KI), Moscow, Russia, Moscow, Russia*
- ³⁷ *Institute of Nuclear Physics, Moscow State University (SINP MSU), Moscow, Russia*
- ³⁸ *Institute for Nuclear Research of the Russian Academy of Sciences (INR RAS), Moscow, Russia*
- ³⁹ *Yandex School of Data Analysis, Moscow, Russia*
- ⁴⁰ *Budker Institute of Nuclear Physics (SB RAS), Novosibirsk, Russia*

- ⁴¹ *Institute for High Energy Physics NRC Kurchatov Institute (IHEP NRC KI), Protvino, Russia, Protvino, Russia*
- ⁴² *ICCUB, Universitat de Barcelona, Barcelona, Spain*
- ⁴³ *Instituto Galego de Física de Altas Enerxías (IGFAE), Universidade de Santiago de Compostela, Santiago de Compostela, Spain*
- ⁴⁴ *European Organization for Nuclear Research (CERN), Geneva, Switzerland*
- ⁴⁵ *Institute of Physics, Ecole Polytechnique Fédérale de Lausanne (EPFL), Lausanne, Switzerland*
- ⁴⁶ *Physik-Institut, Universität Zürich, Zürich, Switzerland*
- ⁴⁷ *NSC Kharkiv Institute of Physics and Technology (NSC KIPT), Kharkiv, Ukraine*
- ⁴⁸ *Institute for Nuclear Research of the National Academy of Sciences (KINR), Kyiv, Ukraine*
- ⁴⁹ *University of Birmingham, Birmingham, United Kingdom*
- ⁵⁰ *H.H. Wills Physics Laboratory, University of Bristol, Bristol, United Kingdom*
- ⁵¹ *Cavendish Laboratory, University of Cambridge, Cambridge, United Kingdom*
- ⁵² *Department of Physics, University of Warwick, Coventry, United Kingdom*
- ⁵³ *STFC Rutherford Appleton Laboratory, Didcot, United Kingdom*
- ⁵⁴ *School of Physics and Astronomy, University of Edinburgh, Edinburgh, United Kingdom*
- ⁵⁵ *School of Physics and Astronomy, University of Glasgow, Glasgow, United Kingdom*
- ⁵⁶ *Oliver Lodge Laboratory, University of Liverpool, Liverpool, United Kingdom*
- ⁵⁷ *Imperial College London, London, United Kingdom*
- ⁵⁸ *School of Physics and Astronomy, University of Manchester, Manchester, United Kingdom*
- ⁵⁹ *Department of Physics, University of Oxford, Oxford, United Kingdom*
- ⁶⁰ *Massachusetts Institute of Technology, Cambridge, MA, United States*
- ⁶¹ *University of Cincinnati, Cincinnati, OH, United States*
- ⁶² *University of Maryland, College Park, MD, United States*
- ⁶³ *Los Alamos National Laboratory (LANL), Los Alamos, United States*
- ⁶⁴ *Syracuse University, Syracuse, NY, United States*
- ⁶⁵ *Laboratory of Mathematical and Subatomic Physics , Constantine, Algeria, associated to²*
- ⁶⁶ *Pontifícia Universidade Católica do Rio de Janeiro (PUC-Rio), Rio de Janeiro, Brazil, associated to²*
- ⁶⁷ *South China Normal University, Guangzhou, China, associated to³*
- ⁶⁸ *School of Physics and Technology, Wuhan University, Wuhan, China, associated to³*
- ⁶⁹ *Institute of Particle Physics, Central China Normal University, Wuhan, Hubei, China, associated to³*
- ⁷⁰ *Departamento de Física , Universidad Nacional de Colombia, Bogota, Colombia, associated to¹⁰*
- ⁷¹ *Institut für Physik, Universität Rostock, Rostock, Germany, associated to¹⁴*
- ⁷² *Van Swinderen Institute, University of Groningen, Groningen, Netherlands, associated to²⁹*
- ⁷³ *National Research Centre Kurchatov Institute, Moscow, Russia, associated to³⁶*
- ⁷⁴ *National University of Science and Technology “MISIS”, Moscow, Russia, associated to³⁶*
- ⁷⁵ *National Research University Higher School of Economics, Moscow, Russia, associated to³⁹*
- ⁷⁶ *National Research Tomsk Polytechnic University, Tomsk, Russia, associated to³⁶*
- ⁷⁷ *Instituto de Física Corpuscular, Centro Mixto Universidad de Valencia — CSIC, Valencia, Spain, associated to⁴²*
- ⁷⁸ *University of Michigan, Ann Arbor, United States, associated to⁶⁴*
- ^a *Universidade Federal do Triângulo Mineiro (UFTM), Uberaba-MG, Brazil*
- ^b *Laboratoire Leprince-Ringuet, Palaiseau, France*
- ^c *P.N. Lebedev Physical Institute, Russian Academy of Science (LPI RAS), Moscow, Russia*
- ^d *Università di Bari, Bari, Italy*
- ^e *Università di Bologna, Bologna, Italy*
- ^f *Università di Cagliari, Cagliari, Italy*
- ^g *Università di Ferrara, Ferrara, Italy*
- ^h *Università di Genova, Genova, Italy*

- ⁱ *Università di Milano Bicocca, Milano, Italy*
- ^j *Università di Roma Tor Vergata, Roma, Italy*
- ^k *Università di Roma La Sapienza, Roma, Italy*
- ^l *AGH — University of Science and Technology, Faculty of Computer Science, Electronics and Telecommunications, Kraków, Poland*
- ^m *LIFAELS, La Salle, Universitat Ramon Llull, Barcelona, Spain*
- ⁿ *Hanoi University of Science, Hanoi, Vietnam*
- ^o *Università di Padova, Padova, Italy*
- ^p *Università di Pisa, Pisa, Italy*
- ^q *Università degli Studi di Milano, Milano, Italy*
- ^r *Università di Urbino, Urbino, Italy*
- ^s *Università della Basilicata, Potenza, Italy*
- ^t *Scuola Normale Superiore, Pisa, Italy*
- ^u *Università di Modena e Reggio Emilia, Modena, Italy*
- ^v *Università di Siena, Siena, Italy*
- ^w *H.H. Wills Physics Laboratory, University of Bristol, Bristol, United Kingdom*
- ^x *MSU — Iligan Institute of Technology (MSU-IIT), Iligan, Philippines*
- ^y *Novosibirsk State University, Novosibirsk, Russia*
- ^z *Sezione INFN di Trieste, Trieste, Italy*
- ^{aa} *School of Physics and Information Technology, Shaanxi Normal University (SNNU), Xi'an, China*
- ^{ab} *Physics and Micro Electronic College, Hunan University, Changsha City, China*
- ^{ac} *Lanzhou University, Lanzhou, China*

- [†] *Deceased*